

The Dark Galaxy Problem and the Effects of Substructure on Gravitational Lenses

R. Benton Metcalf
Institute of Astronomy
Madingley Road
Cambridge CB3 0HA
England

Abstract. I argue that the cold dark matter (CDM) model requires that even within a few kpc of the center of a galactic halo a significant fraction (greater than a few percent) of the surface density is contained in substructures with masses $\gtrsim 10^3 M_\odot$. These structures should be light enough to avoid dynamical friction and dense enough to avoid tidal disruption. I then show using the results of numerical simulations that this substructure will significantly alter the flux ratios of multiply imaged quasars (QSOs) without changing the image positions. The degree to which this occurs will depend on the angular size of the QSO and thus the wavelength of the observations.

1 Introduction

The Λ CDM model of structure formation has so far been enormously successful in explaining the large scale structure of the universe and the anisotropies in the cosmic microwave background (CMB). However the model appears to face some difficulties explaining observations on galactic and smaller scales. A number of such problems have been discussed in the literature [13, 6, 2, 15, for example]. For the present discussion the most relevant of these problems is the observation that CDM simulations of the local group of galaxies predict an order of magnitude more dwarf galaxy halos with masses greater than $\sim 10^8 M_\odot$ than are observed [12, 7, 9]. This could be a sign that there is something fundamentally wrong with the CDM model [1, 4, 5]. Alternatively, the small DM clumps could exist, but not contain observable dwarf galaxies. This situation can easily, perhaps inevitably, come about through the action of feedback processes in the early universe. For example, photoionization can prevent gas from cooling and thus inhibit star formation in small halos [3]. In section 2, I show that the overabundance of DM clumps with respect to visible galactic satellites is likely to extend down to smaller masses and larger fractions of the halo mass than have thus far been accessible to numerical simulations.

These nearly pure dark matter structures have largely been considered undetectable (see [16] for a review of possible methods). Acting as individual gravitational lenses clumps with velocity dispersions of 10 km s^{-1} (corresponding to a mass of order $10^8 M_\odot$) rarely create multiple images and when they do the image separations are too small to be resolved (milli-arcseconds) and are not variable on an observable time scale. However, as shown in [10], if the CDM model is correct and these substructures exist within the lenses responsible for multiply imaged QSOs they will have a dramatic effect on the image magnifications. This is the subject of section 3.

2 The abundance of small mass substructure

In the CDM model galaxy halos are built through the merger of smaller halos. The larger of these subclumps ($\lesssim 10^9 M_\odot$) sink into the center of the halo through the action of dynamical friction where they are destroyed by tidal forces. The orbits of smaller clumps decay much less quickly, but they will suffer tidal stripping and collisions. The Nbody simulations of Klypin *et al.* [7] and Moore *et al.* [12] have shown that substructures of masses $\gtrsim 10^7 M_\odot$ do survive in significant numbers in galactic halos. Within the virial radius of a galactic halo roughly 10% to 15% of the mass is contained in such subclumps. Here I consider how many smaller mass subclumps will survive.

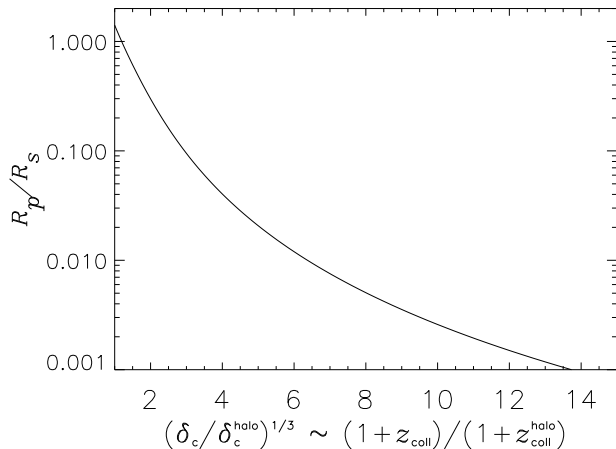


Figure 1: The penetration depth of a subclump as a function of the collapse redshift of the subclump, z_{coll} , and the collapse redshift of the host halo, z_{coll}^{halo} . The scale size of the host halo is R_s (about 20 kpc for the Milky Way).

Navarro, Frenk & White [14] (NFW) found that CDM clumps in their simulations have universal spherically averaged profiles of the form

$$\rho(r) = \frac{\rho_{crit}\delta_s}{(r/r_s)(1+r/r_s)^2}. \quad (1)$$

Once the cosmological parameters and the initial spectrum of density fluctuations have been chosen the NFW profile is approximately a one parameter family; we can consider r_s to be a function of δ_s . There is a significant scatter about this relation however. In agreement with the spherical collapse model the central density is found to be proportional to the average density of the universe at the time when the clump became nonlinear, the collapse time, so $\delta_s \propto (1+z_{coll})^3$.

Clumps orbiting within a larger halo will have mass stripped off them until their radius reduces to approximately the tidal radius, r_t , defined by

$$r_t(\delta_s, R, \delta_s^{halo}) = R \left(\frac{m(r_t)}{M(R)} \right)^{1/3} \left[3 - \frac{\partial \ln M}{\partial \ln R} \right]^{-1/3} \quad (2)$$

where $M(R)$ is the mass of the host halo interior to R and $m(r)$ is the same for the subclump. The superscript “halo” refers to the host halo. It was shown in [10] that while the tidal radius is larger than the subclump scale length, r_s , tidal stripping does not remove a significant amount of mass from the subclumps. With this in mind a penetration depth, R_p , can be defined by the relation

$$r_t(\delta_s, R_p, \delta_s^{halo}) = r_s(\delta_s). \quad (3)$$

At galactic radii $R \lesssim R_p$ mass is transferred between the substructures and a smoother component of DM. Since subclumps are not generally on circular orbits R_p should be thought of as the smallest pericenter distance a clump can have during its orbits without losing much of its mass. It turns out that R_p can be expressed in terms of just $\delta_s/\delta_s^{halo} = (1+z_{coll})^3/(1+z_{coll}^{halo})^3$. The penetration depth is plotted in figure 1. It can be seen there that if $(1+z_{coll})/(1+z_{coll}^{halo}) \sim 3$ or larger the subclump can remain intact down to within a few kpc from the center of the host halo. If we are interested in a galactic halo that is assembled at $z_{coll}^{halo} \sim 1$ then a small mass clump that formed at $z_{coll} \gtrsim 6$ is likely to survive within it.

How plentiful should such subclumps be? The merger history of a halo can be calculated using the extended Press-Schechter formalism [8]. Figure 2 shows what fraction of the mass in a typical galactic halo at $z = 0.6$ is in separate clumps of a given mass range at higher redshifts. The collapse of a typical galaxy halo of mass $\sim 10^{12} M_\odot$ becomes nonlinear at $z \sim 1$ in the $\Omega_{matter} = 0.3$, $\Omega_\Lambda = 0.7$ model used here. Fifty percent of this halo is in clumps of mass $m \lesssim 10^6 M_\odot$ at $z = 6$ which must have undergone collapse at some earlier time (typically this mass scale collapses at $z \sim 7$ though in the overdense region surrounding the future large halo the mean z_{coll} could be larger). Even at $z = 2$, 15% of the final halo is in free floating clumps of $m \lesssim 10^7 M_\odot$ which typically collapsed before $z \sim 6$.

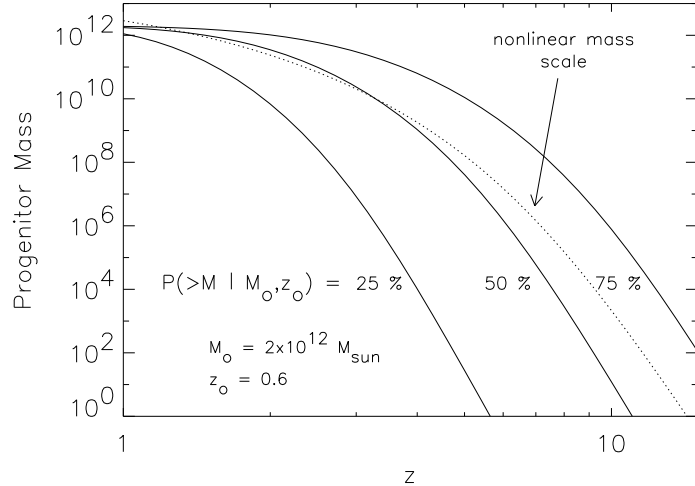


Figure 2: This plot concerns the distribution of progenitors of a halo that is $2 \times 10^{12} M_{\odot}$ at $z = 0.6$. The given fraction (25%, 50% and 75%) of the halo mass is contained in clumps of masses smaller than the curve at the given redshift. For example, 75% of the mass that will end up in the halo is contained in separate clumps with masses $< 10^6 M_{\odot}$ at $z = 10$. Plotted as a dotted curve is the typical mass of objects undergoing nonlinear collapse.

It is difficult to imagine how all this very compact substructure could be efficiently destroyed within the final halo. Collisions are not effective because they are rare and generally at too high a speed to disrupt the clumps. Even when (3) is violated the loss of mass in substructure is a steeper, but still gradual function of R . In addition, the observational constraints on dark satellites of the Milky Way are rather weak in this mass range [10]. As a result I think it is reasonable to assume that at least several percent, perhaps significantly more, of the surface density at a projected radius of $R \sim \text{kpc}$ is contained in substructure. A firmer prediction will ultimately require simulations with mass resolutions several orders of magnitude smaller than are now available.

3 Compound gravitational lensing

Although the gravitational pull on a light beam from a $m \lesssim 10^9 M_{\odot}$ DM clump is very weak, if the beam also passes through a larger mass concentration the contributions to the magnification from the two structures will combine nonlinearly and enhancing the influence of the smaller clump. With the larger lens producing multiple images the effects of the small clumps can be seen in the magnification ratios. For this to happen the angular size of the source cannot be much larger than that of the substructures. QSOs are the obvious choice.

The large number of subclumps and the small, but not vanishingly small, size of the source make numerical simulations of the lensing necessary. Generally an image is influenced by several subclumps acting together rather than an individual one. As a simple example we consider a singular isothermal sphere (SIS) for the primary lens, $M(R) \propto R$. Two images are formed, one farther from the center of the lens, image 1, and one closer, image 2. Image 2 is reversed in one dimension with respect to image 1 and the original source. The Einstein ring radius which characterizes the image separations is $r_E = 4\pi(\sigma_{\text{halo}}/c)^2 D_{\text{ls}} D_1 / D_s$ on the lens plane. D_s , D_1 and D_{ls} are the angular size distances to the source, the lens and between the source and lens. The one-dimensional velocity dispersion of the host halo is σ_{halo} . In a flat $\Omega_{\text{matter}} = 0.3$ model $r_E = 3.5 h^{-1} \text{kpc}$ or 0.3 arcseconds for a lens with $\sigma_{\text{halo}} = 150 \text{ km s}^{-1}$ at $z = 1$ and a source at $z = 3$.

In our simulations the subclumps are positioned randomly, but with an average number density proportional to the total surface density of the primary lens. They are truncated at the tidal radius appropriate for their internal structure and position. This neglects the fact that subclumps may be on elliptical orbits which have taken them closer to the center halo in the past. The mass spectrum of the clumps is taken to be $dN/dm \propto m^{-2}$ in accordance with numerical simulations that extend down to $10^7 M_{\odot}$. The lower mass cutoff in the simulations is effectively set by the smallest mass that can

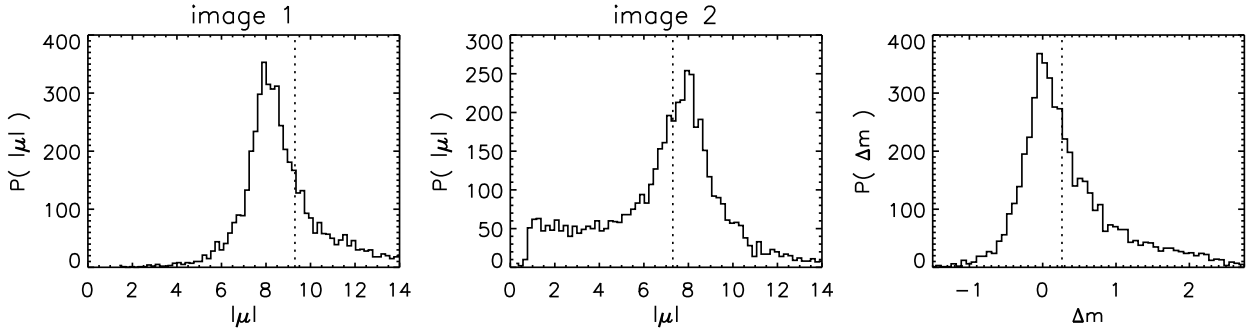


Figure 3: The two panels on the left are the magnification distributions for the two images of a QSO at $z = 3$ lensed by a singular isothermal sphere at $z = 1$. On the right is the distribution of magnification ratios expressed in magnitudes, $\Delta m \equiv 2.5 \log(|\mu_1|/|\mu_2|)$. The subclumps have masses of $10^4 M_\odot < m < 10^8 M_\odot$ and constitute 5% of the halo surface density. The vertical lines show the values expected for the same lens without substructure. The source is at a projected distance of 0.12 Einstein ring radii from the center of the lens. The source is 10 pc in radius. 5,000 realizations are shown.

have a significant effect on the lensing,

$$m_c \simeq \frac{2c^3 R}{\sqrt{3} G \sigma_{\text{halo}}} \left(\frac{l_s}{4\pi D_{\text{ls}}} \right)^{3/2} \quad (4)$$

where l_s is the proper size of the source. Because of this cutoff the source size dictates what mass scales are being probed by compound lensing. For the same example used before $m_c \simeq 10^4 M_\odot (l_s h/\text{pc})^{3/2}$ at $R = 1$ kpc. The broad-line region of a QSO is believed to be a few pc in size. For a more detailed description of these numerical simulations see [10].

The simulations show that the centroid positions of the images are not change significantly by the substructure unless they happen to lay very near a subclump of mass $\sim 10^8 M_\odot$ or larger which is a rare occurrence. Because of this the image positions can still be used to constrain the overall shape of the halo. The resulting “smooth model” can then be used to predict the magnification ratios of quadruply imaged QSOs. This is a more difficult task than might be assumed because smooth models that fit the positions well are usually highly degenerate, predicting a large range of magnification ratios. However, progress has been made in this direction which will be reported elsewhere [11, 18].

Sample magnification and magnification ratio probability distributions are shown in figure 3. These are produced by creating random realizations of the subclump positions and masses. Images 1 and 2 are affected differently by the substructure. This is a result of the one dimensional parity flip of image 2. The most likely μ is biased in opposite directions for the two cases which makes the magnification ratio biased low; that is closer to equal magnification. Negative values of Δm are cases where the order of brightness is the opposite of what is expected from the smooth model. The spread in Δm is quite large compared to typical observational errors, ~ 0.01 mag. In this example Δm is more than 0.2 mag from the smooth model in 74% of the cases. Note that subclumps contain only 5% of the surface density in this example. With sufficiently secure smooth models the absence of such substructure would be clear in the existing sample of quadruply imaged QSOs if it were not for microlensing by ordinary stars.

There are other approaches to detecting compound lensing that could also be pursued. One is to look at the statistics of QSO magnification ratios in general. Substructure will create an overabundance of near equally magnified images. Substructures will also deform multiply imaged radio jets on milli-arcsecond scales. The images can be comparing for signs of small scale distortions that are inconsistent with a smooth lens. These approaches are discussed further in [10].

4 Discussion

The continuum emission region of a QSO in visible wavelengths is very small ($\lesssim 1,000$ AU) and as a result it is susceptible to microlensing by ordinary stars. It has been established that microlensing does cause changes in the image brightness of Q2237+0305 as large as a magnitude [17]. This could

potentially wash out any signal from DM substructures. Fortunately the emission in radio and in atomic and molecular lines are believed to come from a larger region. Variability in the QSO could also be a complication. The time delays between images range from a fraction of a day to months. As long as the source is more than a light-month in size it should not vary on a timescale that would interfere with these investigations. These considerations demonstrate the need for magnification ratios measured in multiple frequencies. With coming data we may soon have a new and unique test of the CDM model.

Acknowledgements. I would like to thank my collaborator on much of this work Piero Madau.

References

- [1] Bode, P., Ostriker, J. P., & Turok, N. 2001, *ApJ*, 556, 93
- [2] Borriello, A. & Salucci, P., 2001, *MNRAS*, 323, 285
- [3] Bullock, J. S., Kravtsov, A. V., & Weinberg, D. H. 2000, *ApJ*, 539, 517; Somerville, R. S., 2001, submitted to *ApJ*(astro-ph/0107507)
- [4] Davé, R., Spergel, D. N., Steinhardt, P. J. & Wandelt, B. D., 2001, *ApJ*, 547, 574
- [5] Kamionkowski, M. & Liddle, A., 2000, *Phys.Rev.Lett*, 84, 4525
- [6] Klypin, A., Kravtsov, A. V., Bullock, J. S., & Primack, J. R. 2001, *ApJ*, 554, 903
- [7] Klypin, A., Kravtsov, A. V., Valenzuela, O., & Prada, F. 1999, *ApJ*, 522, 82
- [8] Lacey, C. & Cole, S., 1993, *MNRAS*, 262, 627
- [9] Mateo, M. 1998, *ARA&A*, 36, 435
- [10] Metcalf, R.B. & Madau, P., 2001, *ApJ* in press, (astro-ph/0108224)
- [11] Metcalf, R.B. & Zhao, H., 2001, in preparation.
- [12] Moore, B., Ghigna, S., Governato, F., Lake, G., Quinn, T., Stadel, J., & Tozzi, P. 1999, *ApJ*, 524, L19
- [13] Moore, B., Quinn, T., Governato, F., Stadel, J., & Lake, G. 1999, *MNRAS*, 310, 1147;
- [14] Navarro, J. F., Frenk, C. S., & White, S. D. M. 1997, *ApJ*, 490, 493
- [15] Sellwood, J., & Kosowsky, A. 2001, in *Gas and Galaxy Evolution (ASP Conf. Series)*, in press (astro-ph/0009074)
- [16] Trentham, N., Moller, O. & Ramirez-Ruiz, E., 2001, *MNRAS* in press (astro-ph/0010545)
- [17] Woźniak, P. R., Alard, C., Udalski, A., Szymański, M., Kubiak, M., Pietrzyński, G. & Zebruń, K., 2000, *ApJ*, 529, 88
- [18] Zhao, H. & Pronk, D., 2001, *MNRAS*, 320, 402